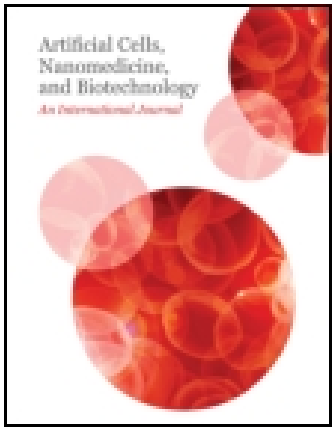

Artificial Cells, Nanomedicine, and Biotechnology: An International Journal

Publication details, including instructions for authors and subscription information:
http://www.tandfonline.com/loi/ianb20

Thermoresponsive biodegradable HEMA-Lactate-Dextran-co-NIPA cryogels for controlled release of simvastatin

Nimet Bölgen[a], Maria Rosa Aguilar[bc], Maria del Mar Fernández[bc], Sandra Gonzalo-Flores[d], Silvia Villar-Rodil[e], Julio San Román[bc] & Erhan Pişkin[f]

[a] Engineering Faculty, Chemical Engineering Department, Mersin University, Mersin, Turkey

[b] Institute of Polymer Science and Technology (ICTP-CSIC), Juan de la Cierva 3, Madrid, Spain

[c] Networking Biomedical Research Center in Bioengineering, Biomaterials and Nanomedicine (CIBER-BBN), Spain

[d] Centro de Biología Molecular Severo Ochoa (CSIC-UAM), Nicolás Cabrera, 1. Campus of the Universidad Autónoma de Madrid, Madrid, Spain

[e] Instituto Nacional del Carbón (INCAR-CSIC), Apartado 73, Oviedo, Asturias, Spain

[f] Chemical Engineering Department and Bioengineering Division, Hacettepe University, Beytepe, Ankara, Turkey

Published online: 18 May 2015.

To cite this article: Nimet Bölgen, Maria Rosa Aguilar, Maria del Mar Fernández, Sandra Gonzalo-Flores, Silvia Villar-Rodil, Julio San Román & Erhan Pişkin (2015) Thermoresponsive biodegradable HEMA-Lactate-Dextran-co-NIPA cryogels for controlled release of simvastatin, Artificial Cells, Nanomedicine, and Biotechnology: An International Journal, 43:1, 40-49, DOI: 10.3109/21691401.2013.837475

To link to this article: http://dx.doi.org/10.3109/21691401.2013.837475

Artificial Cells, Nanomedicine, and Biotechnology, 2015; 43: 40–49

ISSN: 2169-1401 print / 2169-141X online
DOI: 10.3109/21691401.2013.837475

informa
healthcare

Thermoresponsive biodegradable HEMA–Lactate–Dextran-co-NIPA cryogels for controlled release of simvastatin

Nimet Bölgen[1], Maria Rosa Aguilar[2,3], Maria del Mar Fernández[2,3], Sandra Gonzalo-Flores[4], Silvia Villar-Rodil[5], Julio San Román[2,3] & Erhan Pişkin[6]

[1]*Engineering Faculty, Chemical Engineering Department, Mersin University, Mersin, Turkey,* [2]*Institute of Polymer Science and Technology (ICTP-CSIC), Juan de la Cierva 3, Madrid, Spain,* [3]*Networking Biomedical Research Center in Bioengineering, Biomaterials and Nanomedicine (CIBER-BBN), Spain,* [4]*Centro de Biología Molecular Severo Ochoa (CSIC-UAM), Nicolás Cabrera, 1. Campus of the Universidad Autónoma de Madrid, Madrid, Spain,* [5]*Instituto Nacional del Carbón (INCAR-CSIC), Apartado 73, Oviedo, Asturias, Spain, and* [6]*Chemical Engineering Department and Bioengineering Division, Hacettepe University, Beytepe, Ankara, Turkey*

Abstract

NIPA and HEMA–lactate–Dextran-based biodegradable and thermoresponsive cryogels were synthesized at different compositions by cryogelation. Chemical and morphological properties of the HEMA–lactate–Dextran-co-NIPA cryogel matrices were demonstrated by FTIR, SEM, and ESEM. Thermoresponsivity of the prepared cryogels was investigated by DSC, imaging NMR, and swelling studies. For possible use of the cryogels in potential bone tissue engineering applications, either hydrophobic simvastatin was embedded, or hydrophilic simvastatin was incorporated in the cryogels. Release profiles of simvastatin delivering cryogel scaffolds depending on their composition, hydrophobicity or hydrophilicity of loaded simvastatin and the medium temperature were demonstrated.

Keywords: cryogels, biodegradable, drug release, thermoresponsive

Introduction

Poly-L-lactide is hydrolytically degradable, hydrophobic, and biocompatible polymer. The biocompatibility and degradability of poly-L-lactide into nontoxic components make it an appropriate polymer for biomedical applications, for example in controlled drug-release systems (Zhou et al. 2013). Dextran is a natural, enzymatically degradable, hydrophilic, and biocompatible polysaccharide (van Dijk-Wolthuis et al. 1997a, Mehvar 2000) and have been used in drug-delivery vehicles (Cadee et al. 2002). Polymethacrylates are used in a number of pharmaceutical and biomedical applications (Chirila et al. 1992, Flynna et al. 2003). Dextran derivatized with L-lactide grafted 2-hydroxyethyl methacrylate (HEMA–LLA–Dextran) is a macromer, that the gels obtained by polymerization of this compound are biodegradable (van Dijk-Wolthuis et al. 1997b). Poly(N-isopropyl acrylamide) (PolyNIPA) is a thermoresponsive polymer with a volumetric phase transition (VPT) around 32°C in water. This VPT can be modified by the incorporation of more hydrophilic or more hydrophobic monomers to the polymeric chain. In recent years, many interests have been focused on smart/intelligent polymeric materials, which can respond to external stimuli, such as temperature and pH, in volume or shape (Zhuo and Li 2003, Zhang et al. 2003).

The aim of tissue engineering is to replace or facilitate the regeneration of damaged tissue by using scaffolds, cells, and bioactive agents (Levenberg and Langer 2004). As active agents are attracting attention to stimulate/trigger bone regeneration statins have been postulated to affect the bone metabolism. It was demonstrated that different statins have a variable effects on bone, while lovastatin and pravastatin exhibit the least effect, simvastatin, atrovastatin, and cerivastatin present great effects (Garrett et al. 2001). The major limitation in the clinical application of statins for bone regeneration is an appropriate delivery system. Oral administration is effective in controlling blood cholesterol levels, but the systemic availability is only ~2.4% far from being the necessary concentration to healing bone defects (Haberstadt et al. 1992). In addition, the injection at the site of bone fracture or defect at the doses required is cytotoxic because the production of cholesterol is reduced dramatically, and cholesterol is necessary to preserve the integrity of the plasmatic membrane of cells (Benoit et al. 2006). The use of simvastatin as a direct bone graft have been investigated (Wong and Rabie 2003, Wong and Rabie 2005). An inverse correlation has been found between simvastatin

Correspondence: Nimet Bölgen, Engineering Faculty, Department of Chemical Engineering, Mersin University, Ciftlikkoy Campus, 33343, Mezitli, Mersin, Turkey. E-mail: nimetbolgen@yahoo.com, nimet@mersin.edu.tr

(Received 8 August 2013; accepted 20 August 2013)

dose and decrease in bone mineral density (Maritz et al. 2001). We demonstrated that the simvastatin-loaded electrospun poly(ε-caprolactone) scaffolds enhanced reconstruction of cranial bone defects in rats (Piskin et al. 2008).

Cryogelation is a technique that have been applied to prepare cryogels which have interconnected/supermacroporous morphology and spongy and flexible structure (Lozinsky et al. 2002). We applied this technique to prepare biodegradable scaffolds for tissue engineering applications mainly for repair of critical sized cranial bone defects (Bölgen et al. 2007, Bölgen et al. 2008, Bölgen et al. 2009, Bölgen et al. 2011, Bölgen et al. 2014).

Healing of large bone defects is still a major challenge in bone repair. A broad range of tissue engineering matrices have been fabricated from both synthetic and natural polymers by using several porous scaffold preparation methods. There is significant challenge in the design of scaffolds that possess interconnected porous structure and ability of biodegradation and to control release of the drugs or bioactive substances such as growth factors.

Considering the requirements for a proper drug-releasing tissue-engineering scaffold, in this study we designed/attempted to prepare thermoresponsive cryogels, which may be used as "smart" scaffolds loaded with simvastatin, as potential in situ tissue engineering material for reconstruction of critical size hard tissue defects. The most widely used member of thermoresponsive polymers is poly(NIPA) which have been used in a wide variety of bio-related interesting applications. Here, we copolymerized NIPA with HEMA–LLA–Dextran macromer to produce cryogels with thremoresponsive properties. This paper presents our results including cryogel properties and simvastatin release from these scaffolds as a function of temperature.

Materials and methods

Materials

HEMA–lactate–Dextran was synthesized by slightly modifying the protocol presented previously (van Dijk-Wolthuis et al. 1997b, Bölgen et al. 2007). *N*-isopropyl acrylamide, *N,N,N′,N′*-tetramethylenediamine (TEMED), *N,N′*-methylene-bis(acrylamide) (MBAAm) and ammonium persulfate (APS) were purchased from Sigma-Aldrich (Germany) and used as received.

Cryogel synthesis and characterization

Cryogel matrices were prepared in tubular shaped glass molds (0.5 cm diameter) by free radical polymerization of NIPA (monomer) and/or HEMA–LLA–Dextran (macromer). The ingredients were mixed at different monomer/macromer (w/w) ratios and named as follows: 100/0 (cryoNIPA), 80/20 (cryoNIPA80), 60/40 (cryoNIPA60), 40/60 (cryoNIPA40), and 0/100 (cryoHLDex) and dissolved in distilled water. The total monomer/macromer concentration within the solution was 6% (w/v). The crosslinker, MBAAm, was incorporated to the reaction vessel at a concentration of 6.6 w% of the total amount of NIPA and the macromer. MBAAm was added to the formulations in order to increase the materials' stability under physiological conditions. Before TEMED (1%, w) was added to the mixture to initiate the reaction, nitrogen was passed through the solution for 15 min and the solution was cooled in an ice bath for 5 min. Then 1% (w) of APS was added to the solution. The reaction mixture was transferred to the glass mold, frozen at −20°C for 1 h, and the frozen samples were transferred to a −12°C bath and kept for additional 16 h, and finally thawed at room temperature. The fabricated cryogel scaffolds were washed to remove the unreacted monomers, macromers, or initiators and freeze dried by a lyophilizer (Telstar, Lyo Alfa-6, Spain).

FTIR analysis

The chemical structure of the cryogels was confirmed by FTIR. The infra-red spectra of the cryogels were obtained with the equipment Spectrum One (Perkin-Elmer) by the technique Attenuated Total Reflection Fourier Transform Infrared Spectroscopy (ATR-FTIR). The spectra were recorded with 32 scans, a resolution of 4 cm^{-1} and at wavelength between 650 and 4000 cm^{-1}.

Scanning and environmental electron microscope (SEM and ESEM)

Cryogels were analyzed in the swollen and dried state using an Environmental Scanning Electron Microscope (ESEM, Philips XL30 microscope) with tungsten filament equipped with Peltier cooling stage. The apparatus operated in the ESEM or SEM mode depending on the type of sample, wet or dry, respectively. Swollen samples were soaked in water and placed into the ESEM chamber. Temperature was fixed at 2°C and pressure inside the microscope was modified from 6.0 to 1.9 Torr to control the dehydration process. The microscope operated at 15.0 kV. Micrographs were obtained at 500× magnification.

Freeze-dried samples were analyzed in the SEM mode. Cryogels were freeze-dried and sputter-coated with gold before the examination. The microscope was operated at 20.0 kV. Micrographs were obtained at 200× and 500× magnification. Freeze-drying was carried out in a Telstar Lyoalfa-10 machine, at a pressure of 0.1 bar.

Swelling degree

In order to determine the swelling behavior, the cryogels were freeze-dried (m_d). Then, they were soaked in distilled water and allowed to swell. The samples were taken at selected time intervals, carefully dried on a paper to remove the excess water from the gel surface and weighed (m_s). The swelling degree (S_r) was calculated according to Eq. (1). Swelling experiments were carried out at 20°C and 37°C to study the thermoresponsive properties of the cryogels.

$$S_r = [(m_s - m_d)/m_d] \quad (1)$$

Imaging NMR

Imaging NMR (iNMR) was used to investigate the changes in porosity as a result of thermoresponsive property of the cryogels. Cylindrical samples measuring 5×4 mm (diameter × height) were dipped in a 0.8 mM Gadolinium oxide solution. To eliminate air bubbles, the vial was

depressurized several times inside a desiccator and was kept under vacuum until used. In order to reduce T_1 and let a decrease in imaging time without T_1 saturation, the medium was doped with Gadolinium oxide which is a paramagnetic compound. NIH Images (NIH, Bethesda, MD) and Bruker Paravision software were used to process the iNMR images. Hahn spin echo images were obtained at different echo times (T_E) of 3.349, 10, 20, 40, 80, and 120 ms, at different temperatures of 18°C, 21°C, 24°C, 28°C, 32°C, 34°C, and 36.5°C. Representative regions were analyzed. Non-homogeneous areas were not considered and the mean signal intensity was measured for each sample, medium, and the background. The iNMR data were fitted to a monoexponential function and extrapolated to $T_E = 0$ to determine the average proton density for each sample and the medium. Apparent porosity was calculated by Eq. (2):

$$P_i(\%) = [(S_i - S_b)/(S_m - S_b)] \times 100 \quad (2)$$

In Eq. (2), P_i represents the apparent open porosity (i.e., open volume within the sample connected to the outside), S_i, S_b, and S_m are the mean signal intensities of sample section, background, and medium, respectively. All experiments were conducted at least in triplicates (Marcos et al. 2006).

Weight loss

Degradation profiles of the cryogels were investigated at 20 and 37°C in PBS (pH 7.4) by measuring the weight loss of the cryogels harvested from the medium at selected time intervals.

The degradation of the cryogels was followed in PBS (pH 7.4). Dry cryogel specimens (cylindrical monoliths 0.5 cm in diameter and 1 cm in height) were placed in vials containing 5 ml PBS buffer, at 20°C or 37°C. At selected time intervals, samples were removed from the medium; washed very gently with water, changing the water twice to remove all the PBS salts; freeze-dried; and weighed to determine the weight loss. Cryogels were placed back into fresh PBS to continue with the degradation experiment.

Volume phase transition determination by differential scanning calorimetry

Volume phase transition (VPT) of the cryogel scaffolds was analyzed by differential scanning calorimetry (DSC) (Perkin-Elmer DSC 7 calorimeter) with a N_2 flow of 50 mL/min. Swollen samples (in water) were sealed in 50 μL aluminum capsules. Thermograms were recorded between 5°C and 80°C at 3°C/min. All samples were incubated at 5°C for 5 min before the analysis. VPT was determined as the maximum of the endothermic peak that presented the thermogram of each sample.

Simvastatin loading and release

Simvastatin was purchased from Fabricante Artemis (Lote SV046/06/2K). It was hydrophobic without any modification, and its hydrophilic form was prepared by the following method: Simvastatin was treated with 0.1 N NaOH and incubated at 50°C for 2 h. Its pH was adjusted to 7.4 and the solution was lyophilized.

Simvastatin was used in two different forms, hydrophilic and hydrophobic. The hydrophilic one was water soluble and therefore it was expected that simvastatin molecules would be homogeneously distributed within the bulk of the polymer phase (which was called here as "simvastatin incorporated cryogels" shortly as "-sic"). While the hydrophobic one, since it does not dissolve in aqueous medium, would be localized on the inner walls of the pores of cryogel structure (which were referred as "simvastatin embedded cryogels" shortly "-sem"). Therefore, we aimed to create two different systems with two different release rates and profiles. The Simvastatin ratio in the cryogels was 20% weight of the polymer. When preparing sic-cryogels we added Simvastatin to the recipe of the polymer solution before cryogelation. When preparing sem-cryogels, hydrophobic form of Simvastatin was dissolved in ethanol and it was embedded on the cryogels by dropping the simvastatin solution.

An in vitro elution method was used to determine the release behavior of simvastatin from the cryogels. The samples (5 mm diameter, 5 mm height) were immersed in vials containing 5 ml of phosphate buffer saline (0.01M NaCl; 0.138M KCl - 0.0027M) (pH = 7.4) and incubated at 25° and 37°C without stirring. For sem-cryogels, lauryl sulfate sodium salt (SDS), about 10% (w/v), which is over the critical micelle concentration of SDS, was added in the release medium to allow the hydrophobic simvastatin molecules' release from the cryogels and go to the inside of the SDS micelles formed. Samples were collected at selected time intervals from the vials for determination of simvastatin released from the cryogels, and the same amount of plain medium was added. An inverse phase HPLC protocol was applied for determination of simvastatin release within the samples, in which a non-polar stationary phase and a more polar mobile phase (i.e., methanol/water (60/40) with a flow rate of 1 ml/min) were used. The system consists of a Perkin-Elmer LC-250 pump, an UV-Vis detector Perkin-Elmer LC-95 (the wave length for measurements: 239 nm), and a Waters μBoundapack C-18 column of 3.9 × 300 mm. All samples were assayed in duplicate at both 25°C and 37°C. The retention times for sic and sem containing samples were 14.5 ± 0.05 min and 7.5 ± 0.02 min (mean ± SD, $n = 150$), respectively. The calibration curves were made with correlation coefficient over 0.9940 in both cases.

Results and discussion

Cryogelation is a method, where the reaction mixture is polymerized at subzero temperatures. During cryogelation, the frozen solvent crystals act as porogen. After the polymerization reaction is completed the system is defrosted and the interconnected macropores form within the liquid solvent while the reacted polymer is present in the pore walls of the synthesized structures (Lozinsky et al. 2002, Bölgen et al. 2007).

In this study, both monomer/macromer and crosslinker reacted in the specified conditions giving rise to opaque, mechanically stable, sponge-like, very elastic, interconnected, and open macroporous structured materials.

FTIR characterization

The chemical structure of the synthesized cryogels was confirmed by FTIR measurements. As shown in Figure 1, the presence of the characteristic bands of Dextran–lactate–HEMA: $\nu_{st\ C=O}$ from the lactate–HEMA group at 1760 cm^{-1} and $\nu_{st\ C\text{-}OH}$ from the dextran group at 1018 cm^{-1}, was observed in the IR spectra of all three cryogels. The typical amide I ($\nu_{st\ C=O}$) and II ($\nu_{st\ CN}$ and ν_{CNH}) bands at 1641 and 1537 cm^{-1}, respectively, and divided bands of symmetric C-H bending from the -$CH(CH_3)_2$ group at 1386 and 1367 cm^{-1} from PNIPAAm were also observed in the IR spectra of all three cryogels.

SEM and ESEM characterization

Morphology of all cryogels was studied by SEM and ESEM. Freeze-dried samples were visualized in the SEM mode of the microscope and a highly macroporous interconnected structure was distinguished (Figure 2). Porosity was homogeneously distributed in the overall surface of all the specimens, presenting a sponge-like morphology with good elasticity and fast swelling–deswelling kinetics (see swelling experiments below). Figure 2b,d,f show a detail of the pore wall at high magnification (2000×): all synthesized cryogels presented polymeric walls, being cryoNIPA80 and cryoNIPA60 walls continuous, however cryoNIPA40 presented micropores connecting the macropores. The micrographs showed that the cryogel composition has a clear effect on pore morphology.

In situ dehydration of the cryogels was carried out inside the ESEM in order to study changes in the morphology of the materials. The pressure inside the chamber of the microscope was slowly decreased allowing the evaporation of the water filling the polymeric structure. A sequence of micrographs of cryoNIPA40 at different degrees of dehydration is shown in Figure 3. When the sample was fully hydrated

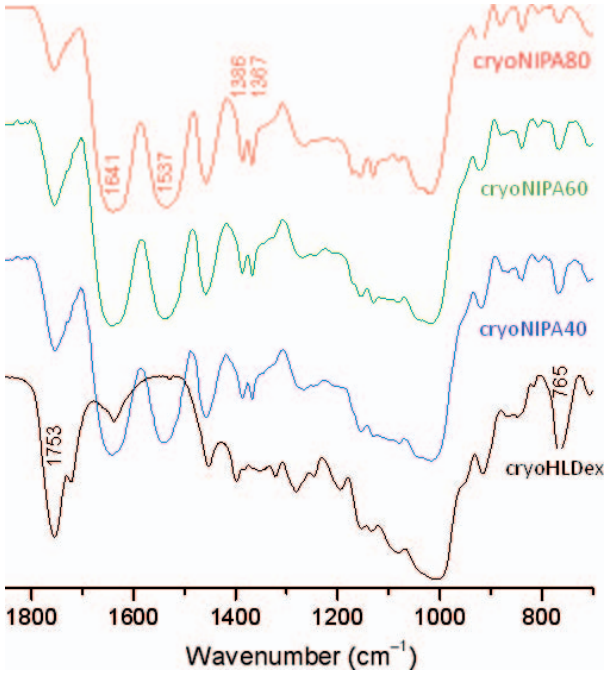

Figure 1. FTIR spectra of the synthesized cryogels.

(Figure 3a), it was impossible to visualize the pores as they were filled with water. As pressure decreased, the water inside the cavities evaporated and the polymeric surface became more visible (Figures 3b and 3c). At high degrees of dehydration, the macroporous structure of cryoNIPA40 cryogel with interconnected pores was more clearly observed (Figure 3d). The macroporous structure of the cryoNIPA40 cryogel was well detected, which demonstrated that the homogeneously distributed porosity was kept after the dehydration of the polymeric matrix. The micropores on the pore walls were only visible when the sample was practically dehydrated (Figure 3d). An increase in the polymeric wall thickness takes place during the hydration of the cryogel, as demonstrated in SEM (Figures 2c and 2d) and ESEM (Figure 3) images.

VPT determination by DSC

VPT of the synthesized cryogels was studied by DSC, getting results only for the cryogels based on cryoNIPA and cryoNIPA80. VPT was very similar for both materials being 29.48°C for cryoNIPA, and 29.38°C for cryoNIPA80 (Figure 4). In the case of those cryogels incorporating higher amount of HEMA–LLA–Dextran in their structure, the change in the heat capacity was too small to be detected by this technique. The unusual low VPT value for cryoNIPA cryogel is in good agreement with the results obtained earlier for similar materials (30.2°C) (Perez et al. 2008) and was explained by the pronounced cryoconcentration of reagents in nonfrozen zones where the polymerization reaction proceeded. The solvent (water) was crystallized, and the polymerization precursors were highly concentrated in a liquid microphase where the polymerization took place. Very thin but dense polymeric walls were formed (Chalal et al. 2009) which favored the macromolecule rearrangement when temperature was raised. In cryoNIPA the polymeric walls shrunk from 12 µm at 23°C to 4 µm at 34°C, and that decrease occurred along the whole range of studied temperatures and not only at the VPT (29.48°C by DSC).

iNMR characterization

There are very few methods that can be used for the characterization of hydrophilic porous materials in their biological environment, such as ESEM, or NMR with freezing out of the solvent and diffusion rate measurements. The former can visualize wet samples in their natural environment, however does not provide an intimate picture of the internal porous structure. The later, does not allow direct investigation of pores, and this information is obtained indirectly. Although information about the porosity of hard porous biomaterials can be obtained by alternative methods such as low temperature, nitrogen adsorption, or mercury porosimetry (Sayil and Okay 2001, Wood and Cooper 2001, Ho et al. 2004), these methods do not allow direct observation of the behavior of these materials in the biological environment, where they normally have a very different structure from that of a dry gel (Plieva et al. 2007). We have published a paper about the characterization of these cryogels by Two-Photon Fluorescence Microscopy (Chalal et al. 2009). A quantitative analysis of the macropore size distribution, and the wall

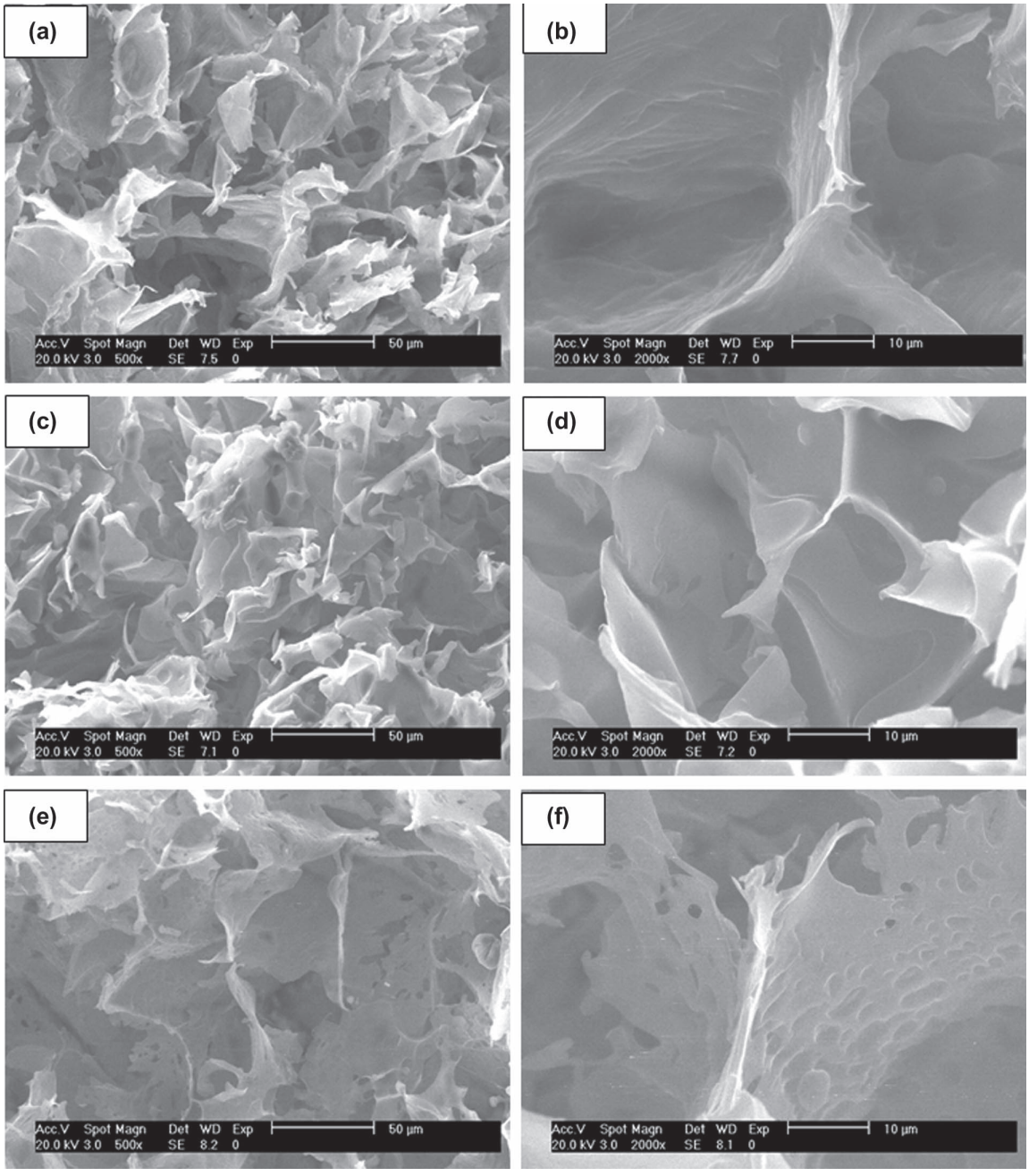

Figure 2. SEM images of cryogels: cryoNIPA80 at (a) 500× and (b) 2000×, cryoNIPA60 at (c) 500× and (d) 2000×, and cryoNIPA40 at (e) 500× and (f) 2000×.

thickness and their modification with respect to the ratio of NIPA/HEMA–LLA–Dextran or to the temperature was demonstrated. However, we also used iNMR to determine different parameters of the swollen cryogels, such as porosity or changes in the dimensions with temperature, in order to contribute to the appropriate characterization of this kind of hydrophilic macroporous soft materials.

iNMR is a non-invasive and non-destructive technique that provides sufficient and adequate information about the porosity of these soft porous materials in situ, in the environment corresponding to their biomedical applications. It is sensitive to molecular level events within fluids, and can spatially resolve fluid states and properties. This technique produces pictures in which the contrast is related to the observable NMR parameters (spin–lattice (T_1) and spin–spin (T_2) relaxation times of the water protons), which are intrinsic to the sample and thereby can provide information about porosity and size of swollen materials. In this work, apparent open porosity of the synthesized cryogels was calculated from measurements of T_2 with experiments conducted on samples saturated with aqueous media. Evolution of size and porosity with temperature was also registered by this technique, and VPT of the cryogel with less content in NIPA was roughly estimated.

Aparent open porosity of cryogels can be determined by iNMR, due to the proportional relation between the intrinsic signal intensity $I_0(w)$, which corresponds to the equilibrium magnetization, that is, the signal obtained in the limit ($T_E \to 0$)

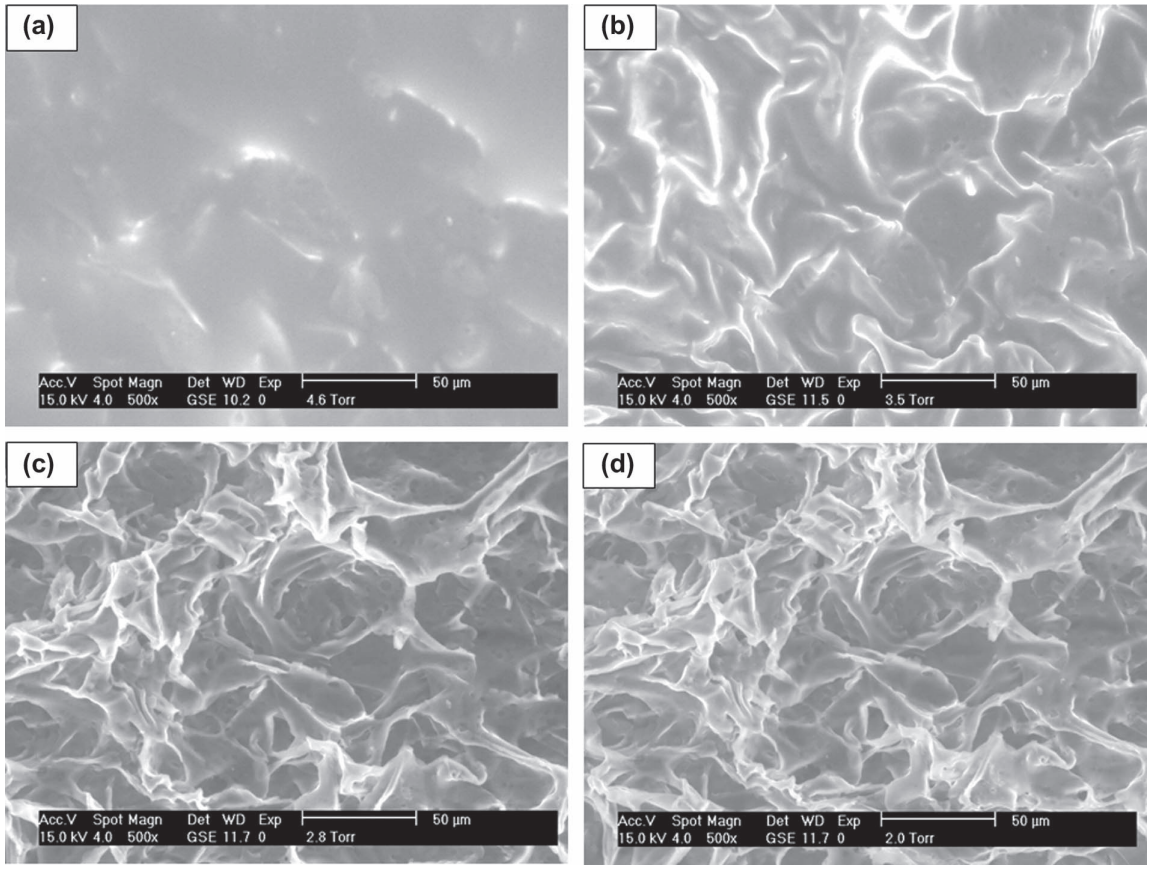

Figure 3. ESEM images of cryoNIPA40. In situ dehydration process. Pressure of the chamber: (a) 4.6, (b) 3.5, (c) 2.8, (d) 2.0 Torr.

and the linear proton density (which can be related to the porosity of the sample) (Kulkarni and Watson 1997, Watson and Chang 1997, Peniche et al. 2013). $I_0(w)$ cannot be measured, however this parameter was estimated by measuring the signal at different degrees of magnetization and doing an estimation of the evolution of the signal intensity with echo time ($I(w,T_E)$), applying Hahn spin echo sequence.

Open porosity of the different materials and its evolution with temperature was calculated. The data shown in Figure 5 for cryoNIPA and cryoNIPA60 presented an intermediate behavior between them. All the analyzed materials presented a highly interconnected porous structure. At temperatures lower than the Lower Critical Solution Temperature of the cryogel, hydrogen bonding between hydrophilic segments of the polymer chain and water molecules dominated, leading to enhanced swelling of the polymer matrix and the expansion of the network (enlarged pore size). However, as the temperature increased, hydrophobic interactions among hydrophobic segments became strengthened, while hydrogen bonding became weaker. The polymer network shrank due to inter-polymer chain association through hydrophobic interactions, and part of the capillary bound water of the cryogel was expelled from the macropores, and pore size

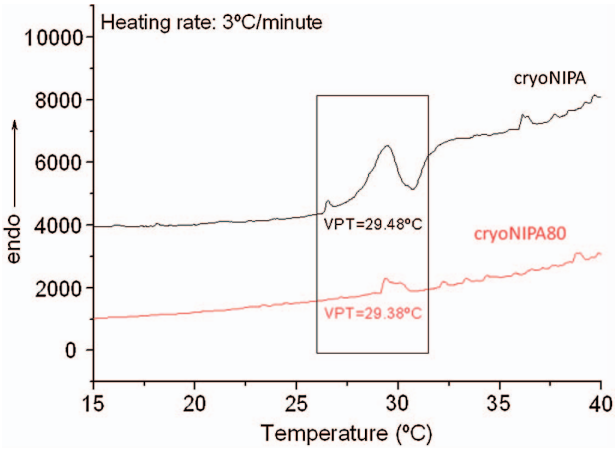

Figure 4. VPT of the synthesized cryogels.

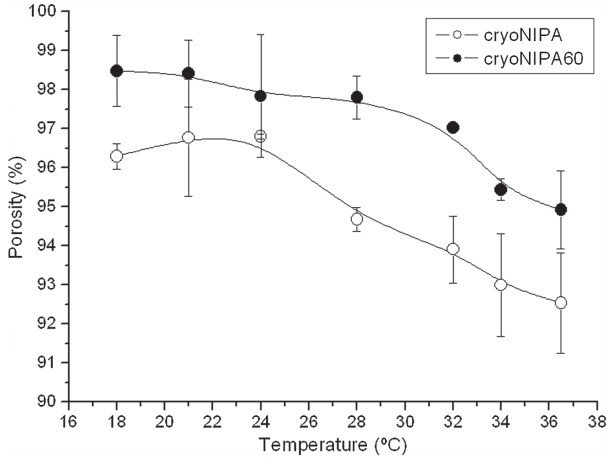

Figure 5. Evolution of open porosity as a function of temperature of cryoNIPA (○) and cryoNIPA60 (●).

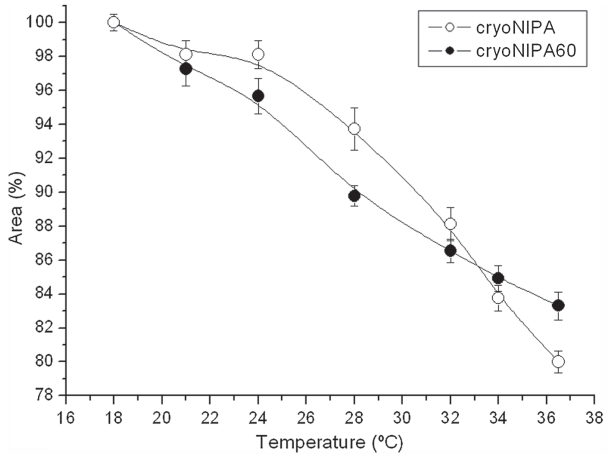

Figure 6. Axial area of cryoNIPA (○) and cryoNIPA60 (●) monoliths as a function of temperature measured by iNMR.

decreased (Qiu and Park 2001). Porosity increased as the content in Dextran–lactate–HEMA increased.

Smart crosslinked polymers undergo a VPT when stimulated. The synthesized cryogels are temperature-sensitive because of the presence of NIPA; however VPT of cryoNIPA60 could not be determined by DSC. The axial area of the cryogels was measured in order to register its evolution with temperature and to see if VPT could be estimated monitoring it. Figure 6 shows the axial area of cryoNIPA and cryoNIPA60 as a function of temperature.

All the synthesized cryogels were T-sensitive and their size decreased with temperature (Figures 6 and 7). CryoNIPA samples remained relatively constant till the temperature was set at 28°C close to the VPT of the cryogel (29.48°C, see DSC characterization). CryoNIPA60 presented a continuous decrease in size with temperature, presenting an inflexion point on the curve around 28°C indicating that VPT of the cryoNIPA60 is close to this temperature.

Swelling experiments

The dependence of swelling degrees on the temperature of the different synthesized cryogels is demonstrated in Figure 8. As the temperature was raised swelling degree decreased. The swelling degree of cryoNIPA40, cryoNIPA60, and cryoNIPA80, decreased from 3152%, 2346%, and 1798% to 1899%, 1333% and 758% when increasing the temperature from 5°C to 40°C, respectively. This behavior was also observed in the cryogel based only on HEMA–LLA–Dextran that passed from 1354% at 5°C to 611% at 40°C. This was attributed to the hydrophilic/hydrophobic nature of this macromonomer which incorporates hydrophobic lactate spacers that were associated when temperature was increased (van Dijk-Wolthuis et al. 1997a). Swelling degree of NIPA/HEMA–LLA–Dextran cryogels increased with an increase in HEMA–LLA–Dextran content. cryoNIPA40 presented the highest swelling degree (3152% at 5°C), while cryoNIPA80 has the smallest swelling degree (1798% at 5°C). Thermosensitivity of polyNIPA-based cryogels is higher than that developed by polyHEMA–LLA–Dextran-based cryogels, and could be related to the slope of the curves in the temperature range between 5 and 25°C (Figure 8).

Very fast changes were observed for these materials as a function of temperature. Thermoresponsive kinetics is controlled by heat transfer within the bulk of the gel and by the solvent diffusion, and hence depends on the geometric dimensions of the specimen. The synthesized materials presented interconnected macroporous morphology, open porosity higher than 90% (see iNMR results), and thin polymeric walls, which favored the heat transfer processes within the pNIPA structure and accelerated the intrinsic time of collapse for these specimens (Lozinsky 2002). The results for the swelling–deswelling experiments of cryoNIPA80 and cryoNIPA60 are presented in Figure 9. Both materials presented a very fast reversible response as the temperature changed from 15°C (T < VPT) to 37°C (T > VPT). Changes in swelling degree were more noticeable in cryoNIPA80 that incorporated higher amount of NIPA monomer in its structure.

Degradation studies

Degradation of the cryogels was studied at 20°C and 37°C in PBS (pH 7.4) and it was found that both the cryogel composition and the temperature played a key role in the degradation profile. The degradation rate increased with increasing HEMA–LLA–Dextran component in their structure, because higher amount of hydrolyzable oligolactate spacers were incorporated in the macromolecular structure.

Figures 10a and 10b show the results for the weight loss of cryogels as a function of degradation time, at 20°C and 37°C, respectively. At higher temperature (37°C), the degradation of cryoNIPA80, cryoNIPA60, and cryoNIPA40 was

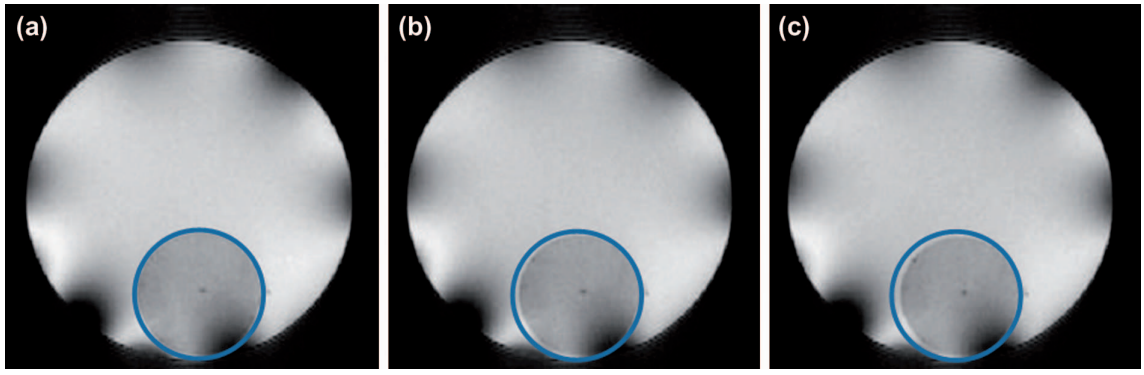

Figure 7. NMR images of polyNIPA80 obtained at 15°C (a), 28°C (b), and 36.5°C (c) and $T_E = 40$ ms.

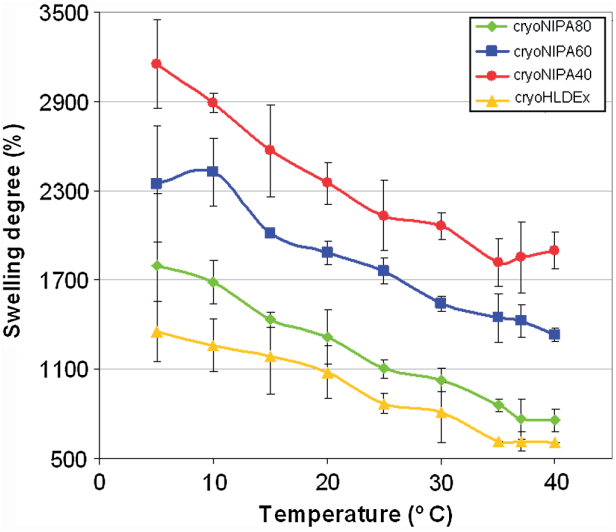

Figure 8. Equilibrium swelling degree of NIPA/HEMA-LLA-Dextran-based cryogels as a function of temperature.

faster than at 20°C. The driving force for the weight loss, that is,the hydrolysis of the oligolactate spacers of the HEMA–LLA–Dextran macromer, was accelerated as a function of temperature. Huang and Lowe (Huang and Lowe 2005) synthesized conventional hydrogels at room temperature with similar chemical composition to our cryogels. They found opposite results in the degradation profiles of their materials: degradation was faster at 20°C (T < VPT) than at 37°C (T > VPT). Conventional thermosensitive gels shrink when temperature is raised over their VPT due to changes in the hydrophilic and hydrophobic interactions between the polymer and the solvent molecules. When polyNIPA hydrogels collapse at T > VPT, a thick skin layer is formed on the surface, which reduces mass transport and isolates the inside of the hydrogel from the outside. This hampers the degradation processes as water cannot penetrate in the bulk of the material. The main difference between these hydrogels and our cryogels is the highly interconnected porous structure obtained under cryogenic conditions, that allows easy heat transfer and mass transport even at T > VPT. An open porosity higher than 90% (see "iNMR characterization", iNMR results), and very thin polymeric walls made easy the hydrolysis of the lactate units at 37°C, even though the thermosensitive cryogels were in the collapsed state.

Release of simvastatin

The percent release of simvastatin (sem and sic) of different formulations and different temperatures (25°C and 37°C), are shown in Figure 11. At 37°C simvastatin release from 80sem and 80sic formulations was significantly greater than 40sem and 40sic, respectively (Figure 11a,b). At this temperature, sic formulations presented a faster release than sem formulations. The same trend was observed at 25°C (Figure 11c,d) for sic formulations; 80sic presented a higher release than 40sic and 60sic, however, the compositional effect was less pronounced. The differences on the release profiles are due to the difference in hydrophilicity between sic (hydrophilic) and sem (hydrophobic). Simvastatin release from sem formulations was around 30% after 10 days, while release from SIC formulations was around 60%–70%.

Between 30% and 40%, embedded simvastatine was released at 25°C, while 25–30% was released at 37°C. In the sem formulations, the hydrophobic form of simvastatin was incorporated on the walls. It seams that interactions between this form of simvastatin and the polymeric matrix exist, as the release profile depended on temperature, it means that it depended on NIPA behavior at temperatures above and below its VPT.

In the sic formulations hydrophilic form of simvastatin was incorporated in the polymeric walls. The release profile

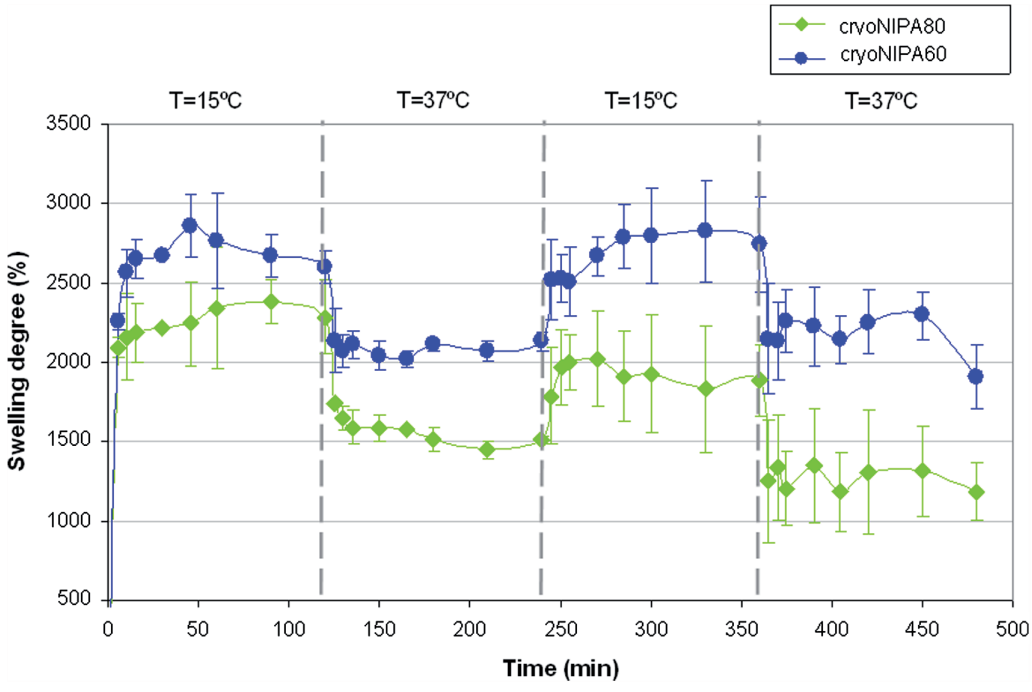

Figure 9. Swelling–deswelling kinetics of cryoNIPA80 and cryoNIPA60 in response to temperature change from 15 to 37°C in water.

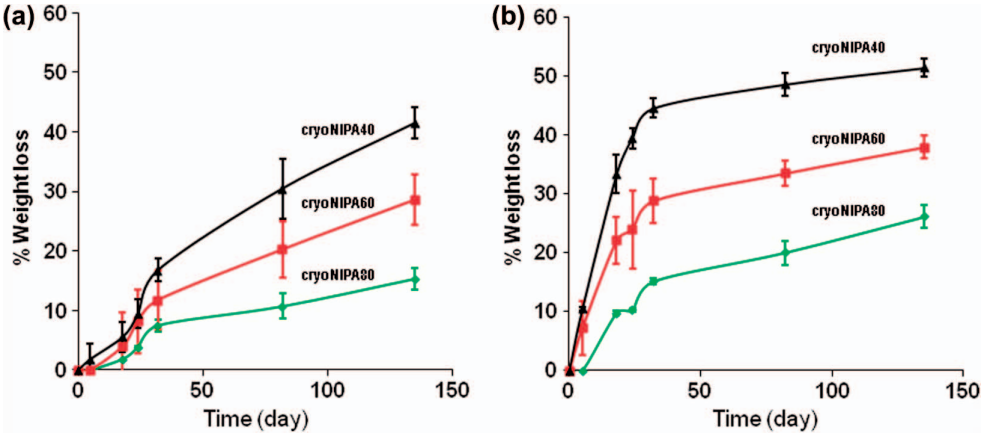

Figure 10. Degradation profiles of cryogels in PBS at (a) 20°C and (b) 37°C.

depended on the structure of simvastatin. This hydrophilic form was easily released to an aqueous medium. The release profile depended on the temperature of the medium and not on the status (swollen or collapsed) of the NIPA-based polymer matrix.

Conclusion

Adjustable biodegradability and a controlled drug-release profile are crucial factors in the design of a tissue engineering scaffold for clinical applications. In this study a new thermoresponsive cryogel containing HEMA–lactate–Dextran-co-NIPA was fabricated to provide a route to control the degradation and simvastatin release. In vitro degradation of the cryogels was affected by the amount of HEMA–lactate–Dextran in the recipe. Release profiles of simvastatin delivering cryogel scaffolds depended on their composition, hydrophobicity or hydrophilicity of loaded simvastatin and the medium temperature.

Several scaffolds that function to release a drug are used for tissue engineering applications. The control of drug release can be obtained by several ways such as using scaffolds prepared from stimuli-responsive polymers or using scaffolds that have adjustable degradation rate or swelling behavior. The cryogel scaffolds fabricated in this study are able to release different amounts of simvastatin depending on the simvastatin-loading method and the medium temperature. The cryogels prepared with different simvastatin loading methods can be used in possible applications as simvastatin delivering scaffolds for regeneration of bone defects. In addition, the simvastatin delivering cryogels, prepared here, may find a potential application to be used

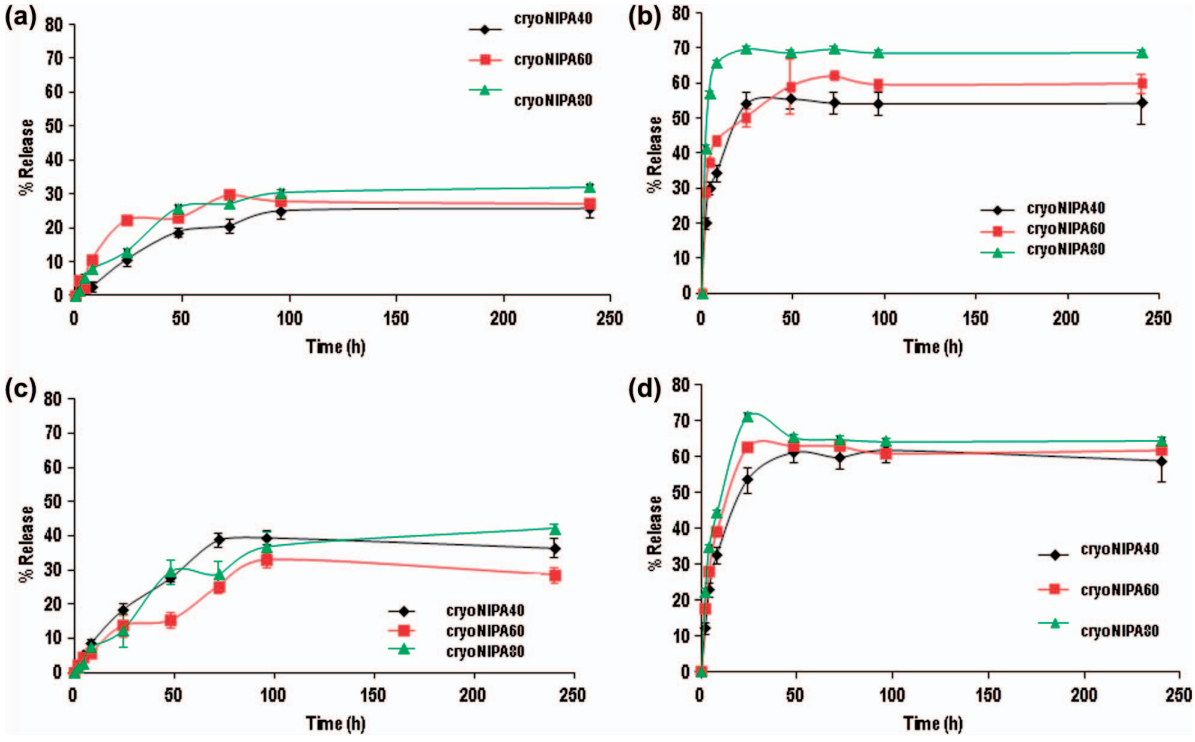

Figure 11. Percent release curves from cryoNIPA40, cryoNIPA60, and cryoNIPA80: at 37° (a) sem formulation, (b) sic formulation; and at 25° (c) sem formulation, (d) sic formulation.

as cell culture construct for osteoblasts; by changing the medium temperature, the simvastatin release rate would change to control the proliferation of osteoblasts. In addition the interconnected macroporous structure of the cryogels would support a well nutrient transport for viable cell maintanence. Further in vitro cell culture or in vivo implantation studies should be conducted.

Acknowledgments

Erhan Pişkin was supported by the Turkish Academy of Sciences (TUBA) as a full member. The authors would like to express their thanks to Dr. Leoncio Garrido for his kind help on the iNMR experiments. Financial support from the NoE. EXPERTISSUES (UE contrac N°: 500283-2), MAT2010-18155 from the Spanish Ministry of Economy and Competitiveness and the "Eugenio Rodríguez Pascual Foundation" project are gratefully acknowledged.

Declaration of interest

The authors report no declarations of interest. The authors alone are responsible for the content and writing of the paper.

References

Benoit DS, Nuttelman CR, Collins SD, Anseth KS. 2006. Synthesis and characterization of a fluvastatin-releasing hydrogel delivery system to modulate hMSC differentiation and fuction for bone regeneration. Biomaterials. 27:6102–6110.

Bölgen N, Plieva F, Galaev IY, Mattiasson B, Pişkin E. 2007. "Cryogelation" for preparation of novel biodegradable tissue engineering scaffolds J Biomat Sci Polym Edn. 18:1165–1179.

Bölgen N, Yang Y, Korkusuz P, Güzel E, El-Haj A, Pişkin E. 2008. Three-dimensional ingrowth of bone cells within biodegradable cryogel scaffolds in bioreactors at different regimes. Tissue Eng Part A. 14:1743–1750.

Bölgen N, Vargel I, Korkusuz P, Güzel E, Pişkin E. 2009. Tissue responses to novel tissue engineering biodegradable cryogel-scaffolds: an animal model. J Biomed Mater Res Part A. 91:60–68.

Bölgen N, Yang Y, Korkusuz P, Güzel E, El-Haj A, Pişkin E. 2011. 3D ingrowth of bovine articular chondrocytes in biodegradable cryogel scaffolds for cartilage tissue engineering. J Tissue Eng Regen Med. 5:770–779.

Bölgen N, Korkusuz P, Vargel I, Kılıç E, Güzel E, Çavuşoğlu T, et al. 2014. Stem cell suspension injected HEMA-Lactate-Dextran cryogels for regeneration of critical sized bone defects. Artif Cells Nanomed Biotechnol. 42:70–77 doi:10.3109/21691401.2013.775578.

Cadee JA, de Groot CJ, Jiskoot W, den Otter W, Hennink WE. 2002. Release of recombinant human interleukin-2 from dextran-based hydrogels. J Control Rel. 78:1–13.

Chalal M, Ehrburger-Dolle F, Morfin I, Vial J, Aguilar de Armas MR, San Roman J, et al. 2009. Imaging the structure of macroporous hydrogels by two-photon fluorescence microscopy. Macromolecules. 42:2749–2755.

Chirila TV, Thompson DE, Constable IJ. 1992. In vitro cytotoxicity of melanized poly(2-hydroxyethyl methacrylate) hydrogels, a novel class of ocular biomaterials. J Biomater Sci Polym Edn. 3:481–498.

Flynna L, Daltona PD, Shoicheta MS. 2003. Fiber templating of poly (2-hydroxyethyl methacrylate) for neural tissue engineering. Biomaterials. 24:4265–4272.

Garrett IR, Gutierrez G, Mundy GR. 2001. Statins and bone formation. Curr Pharm Des. 7:715–736.

Haberstadt C, Anderson P, Bartel R, Cohen R, Naughton G. 1992. Physiological cultured skin substitutes for wound healing. Mater Res Soc Symp Proc. 252:323–330.

Ho MH, Kuo PY, Hsieh HJ, Hsien TY, Hou LT, Lai JY, Wang DW. 2004. Preparation of porous scaffolds by using freeze-extraction and freeze-gelation methods. Biomaterials. 25:129–138.

Huang X, Lowe TL. 2005. Biodegradable thermoresponsive hydrogels for aqueous encapsulation and controlled release of hydrophilic model drugs. Biomacromolecules. 6:2131–2139.

Kulkarni R, Watson AT. 1997. Robust technique fot quantification of NMR imaging data. AIChE J. 43:2137–2140.

Levenberg S, Langer R. 2004. Advances in tissue engineering. Curr Top Dev Bio. 61:113–134.

Lozinsky V, Plieva FM, Galaev YU, Mattiasson B. 2002. The potential of polymeric cryogels in bioseparation. Bioseparation. 10:163–188.

Lozinsky V. 2002. Cryogels on the basis of natural and synthetic polymers: preparation, properties and application. Russ Chem Rev. 71:489–511.

Marcos M, Cano P, Fantazzini P, Garavaglia C, Gomez S, Garrido L. 2006. NMR reflexometry and imaging of water absorbed in biodegradable polymer scaffolds. Magn Reon Imaging. 24:89–95.

Maritz F, Conradie M, Hulley P, Gopal R, Hough S. 2001. Effect of statins on bone mineral density and bone histomorphometry in rodents. Arterioscler Thromb Vasc Biol. 21:1565–1566.

Mehvar R. 2000. Dextrans for targeted and sustained delivery of therapeutic and imaging agents. J Control Rel. 69:1–25.

Peniche H, Reyes-Ortega F, Aguilar MR, Rodríguez G, Abradelo C, García-Fernández L, et al. 2013. Thermosensitive macroporous cryogels functionalised with bioactive chitosan/bemiparin nanoparticles. Macromol Biosci. 19: DOI: 10.1002/mabi.201300184

Perez P, Plieva F, Gallardo A, San Roman J, Aguilar MR, Morfin I, et al. 2008. Bioresorbable and nonresorbable macroporous thermosensitive hydrogels prepared by cryopolymerization. Role of the crosslinking agent. Biomacromolecules. 9:66–74.

Plieva FM, Galaev IY, Mattiasson B. 2007. Macroporous gels prepared at subzero temperatures as novel materials for chromatography of particulate-containing fluids and cell culture applications. J Sep Sci. 30:1657–1671.

Piskin E, İşoğlu İA, Bölgen N, Vargel İ, Griffiths S, Çavuşoğlu T, et al. (2008). In vivo performance of simvastatin-loaded electrospun spiral-wound polycaprolactone scaffolds in reconstruction of cranial bone defects in the rat model. J Biomed Mater Res Part A. 90:1137–1151.

Qiu Y, Park K. 2001. Environment-sensitive hydrogels for drug delivery. Adv Drug Del Rev. 53:321–339.

Sayil C, Okay O. 2001. Macroporous poly(N-isopropyl) acrylamide networks: formation conditions. Polymer. 42:7639–7652.

van Dijk-Wolthuis WNE, Hoogeboom JAM, van Steenbergen MJ, Tsang SKY, Hennink WE. 1997a. Degradation and release behaviour of dextran-based hydrogels. Biomacromolecules. 30: 4639–4645.

van Dijk-Wolthuis WNE, Tsang SKY, Kettenes-van den Bosch JJ, Hennink WE. 1997b. A new class of polymerizable dextrans with hydrolyzable groups: hydroxyethyl methacrylated dextran with and without oligolactate spacer. Polymer. 38:6235–6242.

Watson AT, Chang CTP. 1997. Characterizing porous media with NMR methods. Prog NMR Spectrosc. 31:343–386.

Wong RWK, Rabie ABM. 2003. Statin collagen grafts used to repair defects in the parietal bone of rabbits. Br J Oral Maxillofac Surg. 41:244–248.

Wong RWK, Rabie ABM. 2005. Early healing pattern of statininduced osteogenesis. Br J Oral Maxillofac Surg. 43:46–50.

Wood CD, Cooper AI. 2001. Synthesis of macroporous polymer beads by suspension polymerization using supercritical CO_2 as a pressure-adjustable porogen. Macromolecules. 34:5–8.

Zhang XZ, Wang FJ, Chu CC. 2003. Thermoresponsive hydrogel with rapid response dynamics. J Mater Sci Mater Med. 14:451–455.

Zhuo RX, Li W. 2003. Preparation and characterization of macroporous poly(*N*isopropylacrylamide) hydrogels for the controlled release of proteins. J Polym Sci Part A Polym Chem. 41:152–159.

Zhou J, Hana S, Dou Y, Lud J, Wang C, He H, et al. 2013. Nanostructured poly(L-lactide) matrix as novel platform for drug delivery. Int J Pharm. 448:175–188.